

Micro-beam Analysis at Tohoku University for Biological Studies

著者	Matsuyama S., Ishii K., Abe S., Ohtsu H., Yamazaki H., Kikuchi Y., Amartaivan Ts., Inomata K., Watanabe Y., Ishizaki A., Barbotteau Y., Suzuki A., Yamaguchi T., Momose G., Imaseki H.
journal or publication title	CYRIC annual report
volume	2005
page range	72-77
year	2005
URL	http://hdl.handle.net/10097/50320

V. 2. Micro-beam Analysis at Tohoku University for Biological Studies

*Matsuyama S.¹, Ishii K.¹, Abe S.¹, Ohtsu H.¹, Yamazaki H.¹, Kikuchi Y.¹, Amartaivan Ts.¹,
Inomata K.¹, Watanabe Y.¹, Ishizaki A.¹, Barbotteau Y.¹, Suzuki A.¹, Yamaguchi T.¹,
Momose G.¹, and Imaseki H.²*

¹Graduate School of Engineering, Tohoku University

²National Institute of Radiological Sciences

Introduction

The nuclear microprobe has been recognized as a powerful tool for analysis of single cell and tissue section in biological and biomedical research¹⁻³). We have developed an in-air micro-PIXE system in collaboration with the Japan Atomic Energy Research Institute (JAERI) Takasaki^{4,5}) and have analyzed bovine aortic endothelial (BAE) cells, rat basophilic leukemia (RBL) cells and tumor cells AH109A implanted into Donryu rat⁶⁻⁸). We have also constructed a nuclear microbeam system at the Dynamitron laboratory of Tohoku University for biological applications in 2002-2003. A spatial resolution less than 1 μm is achieved with a beam current of 40 pA^{9,10}). A simultaneous PIXE, RBS and a consecutive STIM analysis can be carried out using in-air or in-vacuum geometry in this system. This system allows to measure structural and elemental properties, which are important for biological studies. However, measurement efficiency of the previous system was not well optimized requiring a long time to obtain sufficient statistics for X-ray and RBS analysis, in particular for low density single cell measurements. Here, we report on a reconfigured detection system with improved detection efficiencies and apply the system to measure spatial distributions of elements in mouse mast cells which are small and difficult to measure using the previous system. Mast cells play an important role in allergic reactions by preserving various kinds of bioactive substances in their secretory granules and releasing them after allergic stimulation. Several bioactive substances are reported to be conjugated with certain metal ions, therefore the elemental distribution of metal ions (including sulfur) inside the cells reflects the distribution of bioactive substances and will help to understand their activity. Although the sample preparation of adhesive cells for PIXE analysis had been already established, we had

not yet established the preparation for non-adhesive cell samples such as mast cell for PIXE analysis. In this study, we established a new sample preparation method suitable for non-adhesive single cell analysis, and undertook first measurements with the improved analysis system.

Microbeam Analysis System

The microbeam analysis system is applicable to experiments using either in-vacuum or in-air PIXE combined with RBS and STIM. Biological applications were mainly carried out using in-air geometry. The previous system consisted of a X-ray detector for PIXE analysis, ion implanted silicon detectors for RBS analysis and on/off axis STM analysis. Technical details of this system were presented in part in previous papers^{9,10}. A schematic diagram of our new in-air analysis system is shown in figure 1. Proton beams are extracted through a thin (a few μm) polymer film, which also serves as a backing for the sample. Three samples are attached on a circular sample holder and can be changed using a stepping motor without breaking the vacuum. To reduce sample damage by the beam and to reduce energy loss in the STIM measurement, He gas was blown on to the sample⁷. Two X-ray detectors are set in vacuum at ± 125 degree with respect to the beam axis. The first one has a large sensitive area (80 mm^2) and is suitable for trace elemental analysis. To reduce pile-up events or deformation of the spectrum by recoil protons, a Mylar filter or a Funny filter can be attached to the front of the detector. Maximum solid angle is ~ 0.08 sr. The second detector has a high-energy resolution (~ 136 eV), a thin Be entrance window ($7.5 \mu\text{m}$) and serves to detect low energy X-rays. The two-detector system enables to detect X-rays ranging from 1 keV to 30 keV with sufficient energy resolution and efficiency in a single measurement.

An annular surface barrier detector is set on the beam axis to detect back-scattered protons for RBS analysis. Scattering angle and counting rates can be controlled by changing the distance between the detector and a sample. The annular detector is highly efficient and improves the solid angle (~ 0.15 sr) without deteriorating angular spread and without interfering with the Si(Li) detectors. The detection efficiency increases 10 times compared to the previous system. Scanning transmission ion microscopy (STIM) can be used to observe the cell morphology. A Silicon PIN-photodiode (Hamamatsu S1223) has been newly installed for charged particle detection. Energy resolution of the Si PIN-photodiode is less than 14 keV and therefore superior to the ion implanted Si detector of larger diameter used in the previous system. The Si PIN-photodiode, a Faraday cup and a scintillator are attached to a detector wheel off center to the beam axis (see Fig. 1). The detector wheel is turned slowly

until the PIN-photodiode is centered on the beam axis, while monitoring the count rate of the detector and reducing beam current accordingly. Sample to detector distance is ~10 mm. Before and after simultaneous PIXE and RBS analysis, STIM data are acquired. Data are acquired in list mode by a multi-parameter data acquisition system. The list mode is very effective to monitor elemental loss during irradiation.

Sample Preparation

Mouse mast cell line P815, which has the characteristic features of non-adhesive type mast cells, was cultured in RPMI 1640 medium supplemented with 10% FBS (Fetal Bovine Serum). After washing three times with THAM (trishydroxymethylaminomethane)-HNO₃ buffer, the cell pellet was resuspended with 15 ml (equivalent to 3 x10⁷ cells) of THAM-HNO₃ buffer and passed through Nuclepore filter of 0.22 μm pore size (Millipore, Isopore Membrane filter). Although trapped cells are not uniformly distributed, the region which is suitable for single cell analysis is found easily. Then, the Nuclepore filter is attached to the 5 μm polycarbonate foil which serves as beam exit window so that cells are inserted between Nuclepore filter and polycarbonate foil. The cells are cryofixed in isopentane solution at liquid nitrogen temperature for 24 hours in vacuum⁶⁻⁸.

Results

The new analysis system was employed. STIM was used to find single cells and proved to be fast and efficient especially when cells are not uniformly distributed. The cell matrix composition (C, N and O), density and thickness were determined by RBS. PIXE provided the elemental information. Typical elemental maps of mast cell are shown in figure 2. It took 90 minutes to obtain the elemental images with beam currents of ~40 pA, a beam spot size of 1×1 μm² and scanning size of 20×20 μm². Quantitative PIXE analysis was performed using the GeoPIXEII software¹¹). Distributions of P, S and K elements are clearly seen and correspond to the C, O maps. Cells keep their original shape and cryofixation seems to be successful. Phosphorus appears to be concentrated in the cell nucleus but S and K are more uniformly distributed through the cell. Iron is strongly localized in one cell only but has been also seen in bovine aortic endothelial (BEA) cells in a previous study¹⁰). The amount of P in a cell is less than 5 pg, which is one half of the RBL cell mass. The improved system is thus capable to measure single cell.

STIM was also used to monitor the loss of cell matrix elements before and after analysis. Typical STIM maps (density maps) are shown in Fig. 3 before and after irradiation.

Before irradiation, cells are clearly seen and correspond to elemental maps. However, cell density is reduced and they are hardly recognized after irradiation. Figure 4 shows the energy loss spectra in the cell at (X 30, Y 50) position in fig.3 and in the backing region around (X 25, Y 13) position before and after irradiation. While the high energy shift corresponding to mass loss is clearly seen in cell region, only peak broadening by increasing inhomogeneity are seen in the backing region. This shows that morphological change has occurred by irradiation, and cell thickness or density is reduced to ~60% of the initial value. The RBS data are consistent with STIM data. However loss of heavy elements ($A > 20$) was not observed in PIXE data indicating that mass loss is from light elements ($A < 20$) only. When mass normalization is needed for analysis, STIM data measured before irradiation should be used even in in-air analysis.

Simultaneous measurements of PIXE, RBS and consecutive STIM employ complementary data and are therefore a powerful tool for cell analysis. We established the preparation method for non-adhesive cells using Nuclepore filter to trap the cells on it for PIXE analysis. This sample preparation has several advantages over the previously reported preparation methods^{3,12}; e.g. 1) the cells which exist in diluted suspension are concentrated, 2) the sample preparation time is short by passing excessive medium through the filter, 3) the recovery of cells used in the preparation is high because most of them are trapped on the filter. These advantages lead to a wide range of applications using non-adhesive cells in micro-PIXE analysis.

Acknowledgements

This study was partly supported by Grant-in-Aid for Scientific Research (S) No. 13852017 from the Ministry of Education, Culture, Sports, Science and Technology, Japan. The authors would like to appreciate the help of K. Komatsu, T. Nagaya and C. Akama in constructing the micro-beam and target system.

References

- 1) Moretto Ph., Llabador Y., Nucl. Instr. Meth. **B130** (1997) 324.
- 2) Labador Y., Moretto Ph., Applications of Nuclear Microprobes in the Life Science, Singapore: World Scientific (1998).
- 3) Hogarth A.N., Thong P.S.P., Lane D.J.W., Watt F., Nucl. Instr. Meth. **B130** (1997) 402.
- 4) Matsuyama S., Ishii K., Sugimoto A., Satoh T., Gotoh K., Yamazaki H., Iwasaki S., Murozono K., Inoue J., Hamano T., Yokota S., Sakai T., Kamiya T., Tanaka R., Int. J. PIXE **8** (1998) 203.
- 5) Sakai T., Hamano T., Hirao T., Kamiya T., Murozono K., Inoue J., Matsuyama S., Iwasaki S., Ishii K., Nucl. Instr. Meth. **B136-138** (1998) 390.
- 6) Ishii K., Sugimoto A., Tanaka A., Satoh T., Matsuyama S., Yamazaki H., Akama C., Amartivan Ts., Endoh H., Oishi Y., Yuki H., Sugihara S., Satoh M., Kamiya T., Sakai T., Arakawa K., Saidoh M.,

- Oikawa S., Nucl. Instr. Meth. **B181** (2001) 448.
- 7) Sugimoto A., Ishii K., Matsuyama S., Satoh T., Gotoh K., Yamazaki H., Akama C., Int. J. PIXE **9** (1999) 151.
 - 8) Tanaka A., Ishii K., Komori Y., Matsuyama S., Satoh T., Gotoh K., Yamazaki H., Akama C., Int. J. PIXE, **12** (2002) 79.
 - 9) Matsuyama S., Ishii K., Yamazaki H., Sakamoto R., Fujisawa, M. Amartaivan Ts, Ohishi Y., Rodoriguez M., Suzuki A., Kamiya T., Oikawa M., Arakawa K., Matsumoto N., Nucl. Instr. Meth. **B210** (2003) 59.
 - 10) Matsuyama S., Ishii K., Yamazaki H., Barbotteau Y., Amartivan Ts., Izukawa D., Hotta K., Mizuma K., Abe S., Oishi Y., Rodrigue M., Suzuki A., Sakamoto R., Fujisawa M., Kamiya T., Oikawa M., Arakawa K., Imaseki H., Matsumoto N., Int. J. PIXE **14** (2004) 1.
 - 11) Ryan C.G., Van Achterbergh E., Yeats C.J., Driberg S.L., Mark G., McInnes B.M., Win T.T., Cripps G., Suter G.F., Nucl. Instr. Meth. **B188** (2002) 18.
 - 12) Ren M.Q., Thong P.S.P., Kara U., Watt F., Nucl. Instr. Meth. **B150** (1999) 179.

Figure 1. Schematic Diagram of the Target Chamber.

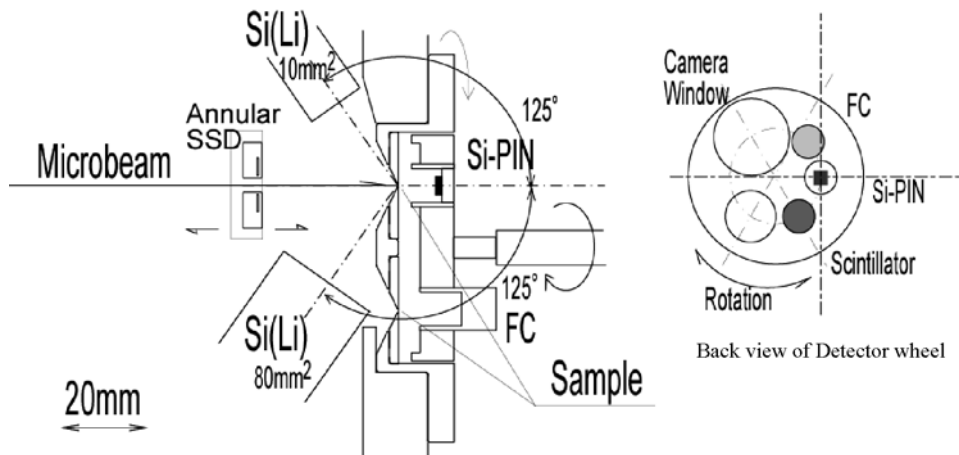
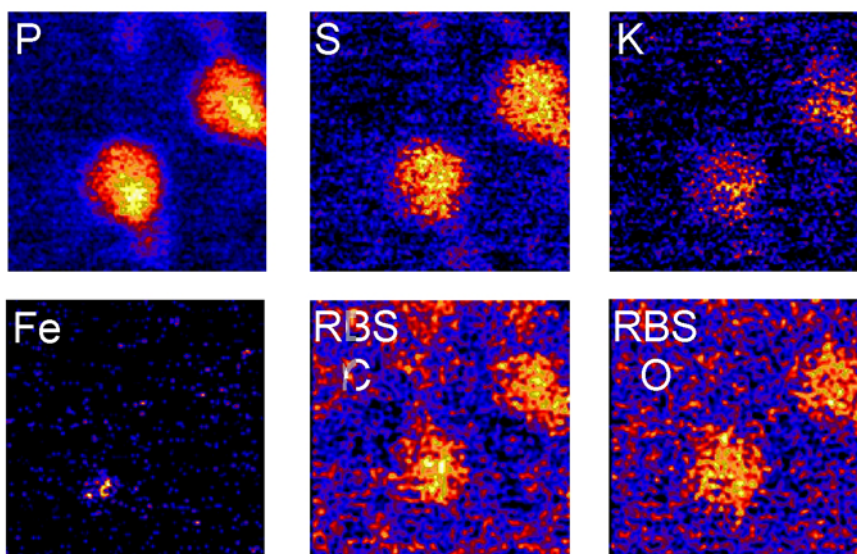


Figure 2. Elemental Maps of Mast Cell. Scanning area is $20 \times 20 \mu\text{m}^2$.



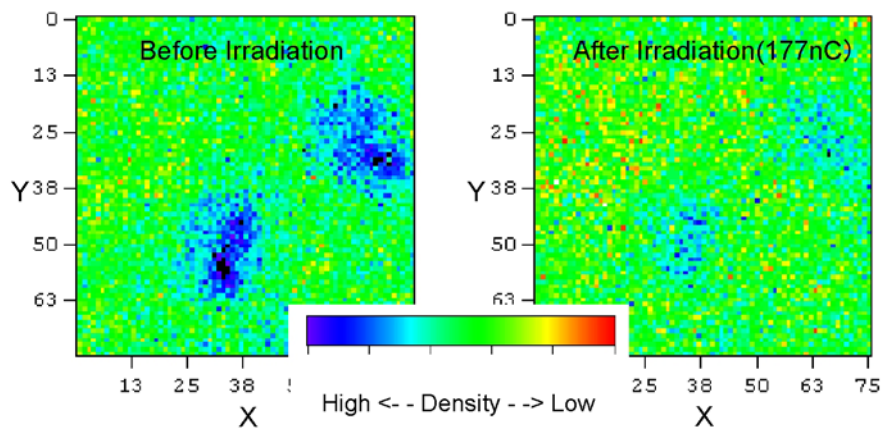


Figure 3. STIM maps before and after irradiation.

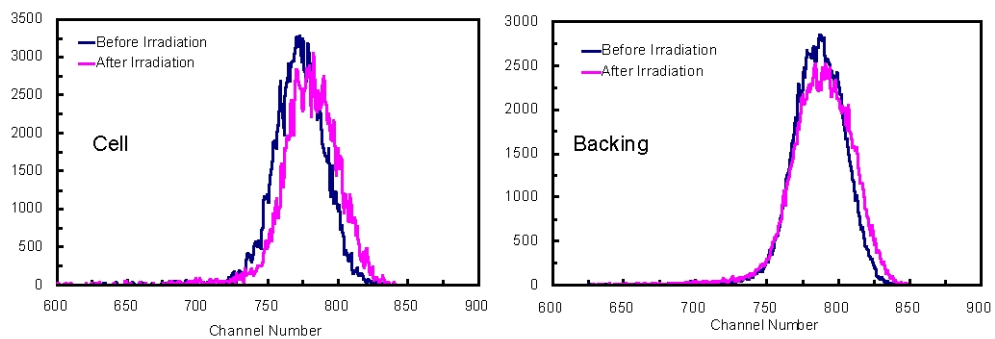


Figure 4. Energy loss spectra in cell at (X 30, Y 50) in Fig. 3 and backing regions around (X 25, Y 13) in Fig. 3 before and after irradiation.